

Stability characteristics for dissipative solitons solutions in three-dimensional complex Swift-Hohenberg equations

GUANGYU JIANG^{a,b,*}, YANJUN FU^{a,b}, KEJUN ZHONG^{a,b}, TIANYI XU^a

^a*School of Measuring and Optical Engineering, Nanchang Hangkong University, Nanchang 330063, China*

^b*Key Laboratory of Nondestructive Testing, Ministry of Education, Nanchang Hangkong University, Nanchang 330063, China*

We investigate the stability characteristics for dissipative solitons solutions in three-dimensional complex Swift-Hohenberg(CSH) equations. The variational approach is used to gain steady state solutions of complex Swift-Hohenberg equations. Following numerical simulations, the quintic-loss parameter, cubic-gain coefficient, effective diffusion (viscosity) or angular spectral filtering have more significant effect on steady state solutions. In particular, an asymmetric input pulses will always give a stable dissipative spatial soliton for dissipative parameters from this domain. The opportunity to achieve analytically and numerically asymmetrical input pulses propagating toward necessarily stable and robust dissipative light bullets opens possibilities for theoretical, experimental and even diverse practical applications.

(Received March 19, 2018; accepted November 29, 2018)

Keywords: Nonlinear optics, Complex Swift-Hohenberg equation, Optical solitons

1. Introduction

Complex Ginzburg-Landau (CGL) equations have drawn more and more attention in physics and applied mathematics communities as a class of universal models that are widely applied in nonlinear optics, fluid dynamics, Rayleigh-Bénard convection, chemical waves, second-order phase transitions, superconductivity, Bose-Einstein condensation and quantum field theories and so on many domains[1-3]. As a dissipative extension of the nonlinear Schrödinger (NLS) equation, the CGL equation exhibit a broad range of unique dynamical behaviors, ranging from chaos and pattern formation[4] to dissipative solitons[5]. Dissipative solitons form continuous families and are supported by the additional balance between linear or nonlinear loss and gain. Moreover, dissipative solitons, including dissipative gap solitons and localized vortices can be stable in the model based on two-dimensional (2D) and three-dimensional (3D) CGL equation with the cubic-quintic (CQ) nonlinearity [6,7]; for a comprehensive review and a recent topical issue on dissipative optical solitons[8-12]. As another dissipative system, the complex Swift-Hohenberg (CSH) equation is derived by adding the four-order diffusion term

to the CGL model [13–15]. The CSH model takes on stronger friction force than the CGL model for the higher-order terms, which lead to some differences between them in optics. Especially, the CSH model also has been widely applied for researching various localized states, including the formation of complex patterns [16] and localized foundational patterns [17-21]. In this paper, we study dissipative solitons solutions in three-dimensional complex Swift-Hohenberg equations(CSH) by using variational and numerical approach. Following numerical simulations, the influence of the quintic-loss parameter, cubic-gain coefficient, effective diffusion (viscosity) or angular spectral filtering steady state solutions has been investigated. These are very helpful for understanding spatiotemporal solitons completely and exploring thoroughly some future potential applications.

2. The model and variational approach

We use the 3D-CQCGL equation to describe the propagation of an electromagnetic field E in the optical medium. In the normalized form [22-25]

$$i \frac{\partial E}{\partial z} + \frac{\partial^2 E}{\partial x^2} + \frac{\partial^2 E}{\partial y^2} + \frac{\partial^2 E}{\partial t^2} + |E|^2 E + \nu |E|^4 E = Q \quad (1)+$$

where ν is the quintic self-defocusing coefficient, δ is the linear loss or gain coefficient, μ denotes quintic-loss parameter, ε is the cubic-gain coefficient, and

β accounts for effective diffusion (viscosity) or angular spectral filtering in the medium. The right-hand side of (1) contains dissipative terms Q , can be expressed by

$$Q = i \left[\delta E + \beta \left(\frac{\partial^2 E}{\partial x^2} + \frac{\partial^2 E}{\partial y^2} + \frac{\partial^2 E}{\partial t^2} \right) + \varepsilon |E|^2 E + \mu |E|^4 E + s \left(\frac{\partial^4 E}{\partial x^4} + \frac{\partial^4 E}{\partial y^4} + \frac{\partial^4 E}{\partial t^4} \right) \right] \quad (2)$$

where s denotes the higher-order parameter. To establish the variational approach for CQGLE, we construct the total Lagrangian of the system described by Eq. (1) and

Eq. (2) containing a conservative and a dissipative part [22]. An asymmetric trial function can be expressed by

$$E = A \exp \left[-\frac{x^2}{2X^2} - \frac{y^2}{2Y^2} - \frac{t^2}{2T^2} + i(Cx^2 + Gy^2 + St^2 + \psi) \right] \quad (3)$$

where the amplitude A , unequal spatial widths X, Y and T , unequal wavefront curvatures C, G and S and phase ψ , all functions change with the longitudinal coordinates z

[22]. Optimization of each of these functions gives one of eight Euler-Lagrange equations averaged over transverse coordinates

$$\frac{d}{dz} \left(\frac{\partial L_C}{\partial \eta'} \right) - \frac{\partial L_C}{\partial \eta} = 2 \operatorname{Re} \iiint Q \frac{\partial E^*}{\partial \eta} dx dy dt \quad (4)$$

where L_C is the conservative Lagrangian and Re denotes the real part [22]. Within the variational approximation, the partial differential CQGLE corresponds a set of eight

coupled first-order differential equations (FODEs) resulting from the variations in amplitude

$$\frac{dA}{dz} = A \left[\begin{aligned} & \delta + \varepsilon A^2 \frac{7}{2R^2 B^2} + \mu A^4 \frac{3}{R^2 B^4} - \beta \left(\frac{1}{X^2} + \frac{1}{Y^2} + \frac{1}{T^2} \right) - 2(C + G + S) \\ & + 3s \left[\frac{3}{4} \left(\frac{1}{X^4} + \frac{1}{Y^4} + \frac{1}{T^4} \right) + 2(C^2 + G^2 + S^2) + 4(C^4 X^4 + G^4 Y^4 + S^4 T^4) \right] \end{aligned} \right] \quad (5a)$$

asymmetric widths

$$\frac{dX}{dz} = 4CX + \left[\frac{\beta}{X^2} - 4\beta C^2 X^2 - \varepsilon A^2 \frac{1}{R^2 B^2} - \mu A^4 \frac{1}{R^2 B^4} - 3s \left(\frac{1}{X^4} + 16C^4 X^4 \right) \right] X \quad (5b)$$

$$\frac{dY}{dz} = 4GY + \left[\frac{\beta}{Y^2} - 4\beta G^2 Y^2 - \varepsilon A^2 \frac{1}{R^2 B^2} - \mu A^4 \frac{1}{R^2 B^4} - 3s \left(\frac{1}{Y^4} + 16G^4 Y^4 \right) \right] Y \quad (5c)$$

and

$$\frac{dT}{dz} = 4ST + \left[\frac{\beta}{T^2} - 4\beta S^2 T^2 - \varepsilon A^2 \frac{1}{R^2 B^2} - \mu A^4 \frac{1}{R^2 B^4} - 3s \left(\frac{1}{T^4} + 16S^4 T^4 \right) \right] T \quad (5d)$$

Anisotropic wave front curvatures

$$\frac{dC}{dz} = \frac{1}{X^4} - 4C^2 - \frac{1}{R^2 B^2 X^2} A^2 - \frac{1}{R^2 B^4 X^2} \nu A^4 - \frac{4\beta C}{X^2} + 12sC \left(\frac{1}{X^4} + 4C^2 \right) \quad (5e)$$

$$\frac{dG}{dz} = \frac{1}{Y^4} - 4G^2 - \frac{1}{R^2 B^2 Y^2} A^2 - \frac{1}{R^2 B^4 Y^2} \nu A^4 - \frac{4\beta G}{Y^2} + 12sG \left(\frac{1}{Y^4} + 4G^2 \right) \quad (5f)$$

and

$$\frac{dS}{dz} = \frac{1}{T^4} - 4S^2 - \frac{1}{R^2 B^2 T^2} A^2 - \frac{1}{R^2 B^4 T^2} \nu A^4 - \frac{4\beta S}{T^2} + 12sS \left(\frac{1}{T^4} + 4S^2 \right) \quad (5g)$$

and phase

$$\begin{aligned} \frac{d\psi}{dz} = & - \left(\frac{1}{X^2} + \frac{1}{Y^2} + \frac{1}{T^2} \right) + \frac{7\varepsilon A^2}{2R^2 B^2} + \frac{3\mu A^4}{R^2 B^4} + 2\beta(C + G + S) \\ & + 6sCX^2 \left(\frac{3}{X^4} - 4C^2 \right) + 6sGY^2 \left(\frac{3}{Y^4} - 4G^2 \right) + 6sST^2 \left(\frac{3}{T^4} - 4S^2 \right) \end{aligned} \quad (5h)$$

where $B = 3^{5/4}/2^{7/4}$, $R = 8/3^{3/4}$. Without higher-order dispersion and diffraction ($s=0$), the model is transformed into the standard CQGL. Only symmetric steady state solutions, with equal widths ($X=Y=T$) and curvatures ($C=S=G$), can exist. To have a stable pulse background, the linear dissipation term has to correspond to a loss, i.e. the parameter δ must always be negative [12]. All remaining dissipative parameters are divided by $\delta_0 = |\delta|$: $\varepsilon_0 = \varepsilon/\delta_0$, $\mu_0 = \mu/\delta_0$, $\beta_0 = \beta/\delta_0$. However, as in

conservative systems, for small chirp, it follows from Eq. (5) that the width $X = RB^2 A^{-1} (B^2 + \nu A^2)^{-\nu/2}$ and the striking difference from conservative systems is the nonzero wave front curvature $C = 0.25R^{-2} B^{-4} A^2 [(\varepsilon_0 - \beta_0)B^2 + (\mu_0 - \beta_0 \nu)A^2 + 3s_0 A^2 (B^2 + \nu A^2)^2] \beta_0$. The beam power $P = A^2 X Y T$ is no more conserved in dissipative systems. Moreover, we get the equation of the corresponding steady state amplitude:

$$4R^4 B^8 + 2R^2 B^4 A^2 [(7\varepsilon_0 - 6\beta_0)B^2 + 6(\mu_0 - \nu\beta_0)A^2] + 27s_0 A^4 (B^2 + \nu A^2)^2 = 0 \quad (6)$$

3. Results and discussion

In this section, we will discuss the properties of dissipative solitons solutions in three-dimensional complex Swift-Hohenberg equations. During the calculations, we select the generic case for the set of parameters [22-25]: $\delta_0 = 0.01$, $\varepsilon_0 = 23$, $\mu_0 = -40$ and $\beta_0 = 5$. Unless otherwise specified, the following calculations are performed using the above parameters. According to the equations of width, wave front curvature and steady state amplitude, the width and wave front curvature can be known when the steady state amplitude strongly depends on quintic-loss parameter, cubic-gain coefficient, effective

diffusion (viscosity) or angular spectral filtering. To evaluate the stability characteristics for dissipative solitons solutions, we analyze the amplitude, peak power and width varying with system parameters. Fig. 1 shows the steady state amplitude, beam power and width as a function of cubic-gain coefficients for different fourth-order diffraction and higher-order spectral filterings. When the higher-order parameter s is -10, the amplitudes taking on bifurcation curve correspond to A^+ and to A^- , respectively. The bifurcation corresponding to A^+ is on the lower unstable branch, the bifurcation associated to A^- is on the upper stable branch. For a small and moderate higher-order parameter s ($=-10$), The amplitude A^+

decreases gradually with increase of the parameter ε_0 , and has a slight difference. However the amplitude A^- is curved and increases gradually with increase of the parameter ε_0 , appears a point of inflexion in curve, then increases with increase of the parameter ε_0 . Moreover when the parameter s is increased to -20 , the amplitude A^- is curved and increases gradually with increase of the parameter ε_0 for given higher-order parameter s , appears a point of inflexion in curve, then increases with increase of the parameter ε_0 . As the parameter s is further increased to -30 and -40 , the amplitude variation is the similar with that for the parameter -20 , but its changes are small, as shown in Fig. 1(a). Fig. 1(b) presents the corresponding peak powers with cubic-gain coefficients for different fourth-order diffraction. Obviously, the peak power is monotonically increasing with increase of the

parameter ε_0 for the amplitude A^+ , it presents various change trends with the parameter ε_0 for the amplitude A^- . When the parameter s is -10 , the peak power decreases gradually, its variation difference is very small after the parameter ε_0 . Similarly the parameter s is further increased, the peak power decreases gradually, its variation difference is very small for the a high parameter ε_0 , finally remains constant. Compared with Fig. 1 (b), the width change trends have the same to these of the peak power for the amplitude A^+ and A^- , as shown in Fig. 1 (c). We can make clear that solitons with the amplitude A^- can be stable with increase of the parameter ε_0 for given fourth-order diffraction s , on the contrary solitons with the amplitude A^+ can be unstable for the same parameters.

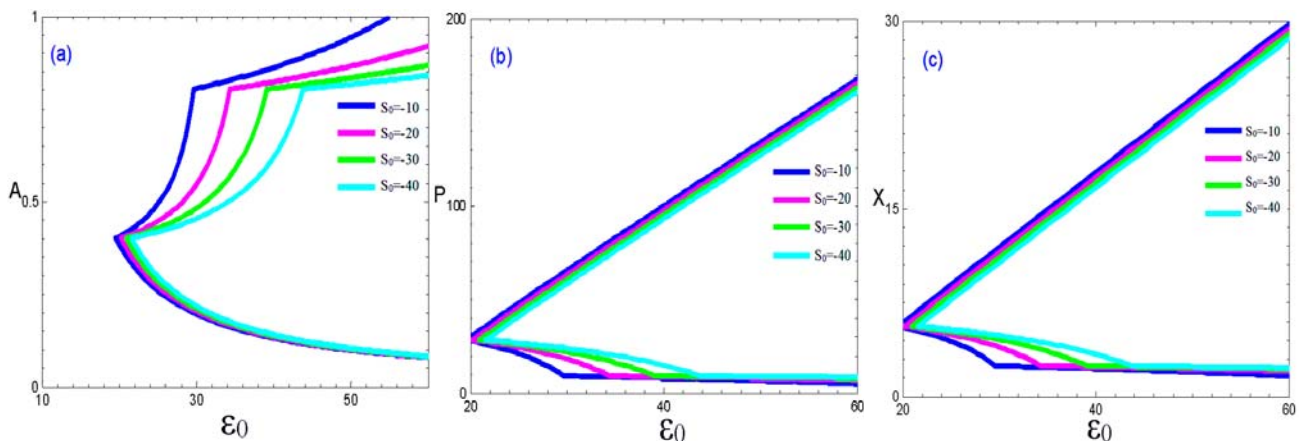


Fig. 1. The stable steady state solutions amplitude A , beam power P and width X with different cubic-gain coefficients

Fig. 2 shows the steady state amplitude, beam power and width changing with cubic-gain coefficients for different fourth-order diffractions and higher-order spectral filterings. The amplitudes A^+ and A^- are on the lower unstable branch and on the upper stable branch respectively. With increase of the parameter μ_0 , the initial amplitude A^+ increase gradually and has a slight difference. However the amplitude A^- decreases gradually, appears a sudden change, and decreases with increase of the parameter μ_0 for different higher-order parameters s . As the parameter s is -10 , the amplitude A^- decreases gradually, then decreases suddenly with increase of the parameter μ_0 . As the parameter s is further increased to -20 , the amplitude variation is the similar with that for the parameter -10 , but its changes are small. As the parameter s

is further increased to -30 and -40 , the amplitude variation is the similar with that for the parameter -10 , but its changes are small, as shown in Fig. 2 (a). Fig. 2 (b) presents the corresponding peak powers with cubic-gain coefficients for different fourth-order diffractions. Obviously, with increase of the parameter μ_0 , the peak power is monotonically increasing for the amplitude A^+ , it presents various change trends with the parameter μ_0 for the amplitude A^- . When the parameter s is -10 , the peak power decreases gradually, its variation difference is very small after the parameter μ_0 . As the parameter s is further increased, the peak power decreases gradually, its variation difference is very small after the a bigger parameter μ_0 , finally keeps constant. Compared with Fig. 2 (b), the width change trends have the same to these of

the peak power for the amplitude A^+ and A^- , as shown in Fig. 2 (c). From these figures, we can see that the amplitude A , the corresponding peak powers and the width have opposite change trends with Fig. 1, solitons with the

amplitude A^- can be stable with increase of the parameter μ_0 for given fourth-order diffraction, on the contrary solitons with the amplitude A^+ can be unstable for the same parameters.

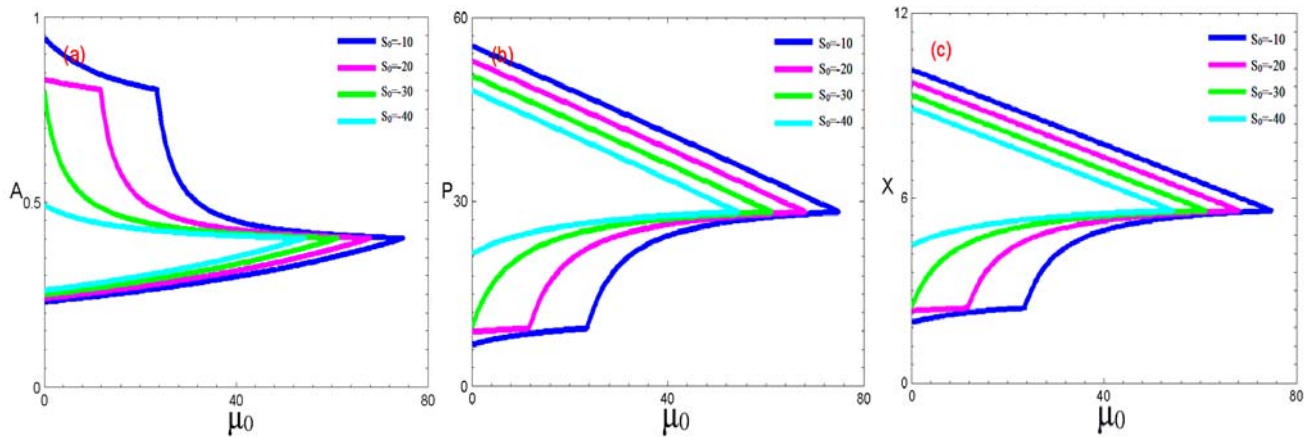


Fig. 2. The stable steady state solutions amplitude A , beam power P and width X with different quintic-loss parameters

To further understand the effect of other system parameters on stability characteristics for dissipative solitons solutions in three-dimensional complex Swift-Hohenberg equations. Fig. 3 shows the steady state amplitude, beam power and width varying with cubic-gain coefficients for different fourth-order diffraction and higher-order spectral filtering. The amplitudes A^+ and A^- are on the lower unstable branch and on the upper stable branch respectively. With increase of the parameter β_0 , the amplitude A^+ increase gradually and has a slight difference. However the amplitude A^- decreases gradually with increase of the parameter β_0 for different higher-order parameter s . As the parameter s is -10, the amplitude A^- decreases gradually, then decreases suddenly with increase of the parameter β_0 . As the parameter s is further increased to -20, the amplitude variation is the similar with that for the parameter -10, but its changes are much smaller. As the parameter s is further increased to -30 and -40, the amplitude variation is the similar with that for the parameter -10, but its changes are small, as shown in Fig. 3 (a). Fig. 3 (b) presents the corresponding peak powers with cubic-gain coefficients for different fourth-order diffraction. We can make clear that the peak power is monotonically increasing with increase of the parameter β_0 for the amplitude A^- , it presents various change trends with the parameter β_0 for

the amplitude A^+ . When the parameter s is -10, the peak power decreases gradually, its variation difference is very small after the parameter β_0 . Similarly the parameter s is further increased, the peak power decreases gradually, its variation difference is very small for a bigger parameter β_0 , finally remains constant. Compared with Fig. 3 (b), the width change trends have the same to these of the peak power for the amplitude A^+ and A^- , as shown in Fig. 3 (c). As the parameter s is -10, the amplitude A^- decreases gradually, then decreases suddenly with increase of the parameter β_0 , as shown in Fig. 3 (d). Fig. 3 (e) presents the corresponding peak powers with cubic-gain coefficients for different fourth-order diffraction. The peak power is monotonically increasing with increase of the parameter β_0 for the amplitude A^- , it presents various change trends with the parameter β_0 for the amplitude A^+ . When the parameter s is -10, the peak power decreases gradually, its variation difference is very small after the parameter β_0 . Similarly the parameter s is further increased, the peak power decreases gradually, its variation difference is very small after the a bigger parameter β_0 , finally keeps unchanged. Compared with Fig. 3 (e), the width change trends have the same to these of the peak power for the amplitude A^+ and A^- , as shown in Fig. 3 (f). We find that the the amplitude, peak powers and width change trends become narrower and narrower

with increase of the parameter β_0 , the effective diffusion (viscosity) or angular spectral filtering in medium is unfavorable for the stable solitons in dissipative solitons

solutions in three-dimensional complex Swift-Hohenberg (CSH) equations.

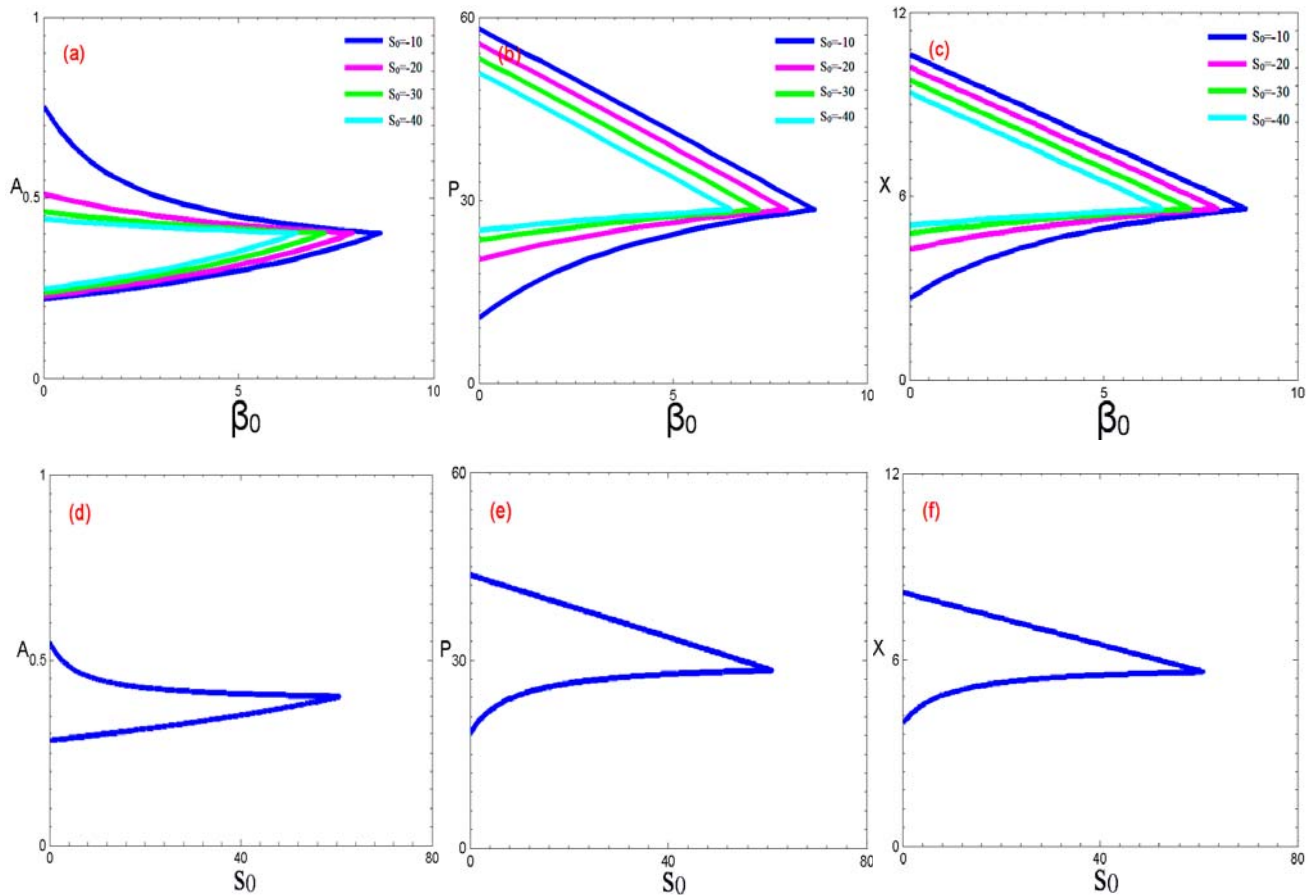


Fig. 3. The stable steady state solutions amplitude A , beam power P and width X with cubic-gain coefficients for different fourth-order diffractions and higher-order spectral filterings.

4. Conclusions

In conclusion, the (3+1)-dimensional CSH equation is treated for an asymmetric input, using numerical and analytical approach. The stable steady-state solutions are obtained analytically through exact parametric resolution. The results show that the quintic-loss parameter, cubic-gain coefficient, effective diffusion (viscosity) or angular spectral filtering have an important effect on steady state solutions. It is worthwhile to stress that even very asymmetric input pulses, which are far from stable spherically symmetric steady states, always self-organize into solitons for the same dissipative parameters. Therefore, bullets are very robust, resisting successive increase of amplitude in the process of evolution. These results suggest potential and practical applications such as routing light signals, all-optical data-processing schemes in optical communication devices, stable and robust dissipative light bullets in nonlinear dissipative media.

Acknowledgements

This work was supported by the National Natural Science Foundation of China (Nos. 11864026 and 61661034) and Natural Science Foundation of Jiang xi Province of China (Grant No. 20161BAB206116).

References

- [1] I. S. Aranson, L. Kramer, *Rev. Mod. Phys.* **74**, 99 (2002).
- [2] B. A. Malomed, *Nonlinear Schrödinger equations*, in: *Encyclopedia of Nonlinear Science*, New York, Routledge, 2005.
- [3] N. N. Rosanov, *J. Opt. B: Quantum. Semiclass. Opt.* **6**, R60 (2004).

- [4] N. Akhmediev, A. Ankiewicz, Lecture Notes in Physics 661, Springer, Berlin, 2005.
- [5] D. Mihalache, D. Mazilu, F. Lederer, H. Leblond, B. A. Malomed, Phys. Rev. A **76**, 045803 (2007).
- [6] D. Mihalache, D. Mazilu, F. Lederer, Y. V. Kartashov et al., Phys. Rev. Lett. **97**, 073904 (2006).
- [7] N. N. Rosanov, S. V. Fedorov, A. N. Shatsev, Lecture Notes in Physics **751**, 93 (2008).
- [8] R. Kuszelewicz, S. Barbay, G. Tissoni, G. Almuneau, Eur. Phys. J. D **59**, 1 (2010).
- [9] Y. J. He, B. A. Malomed, F. Ye, B. Hu, J. Opt. Soc. Am. B **27**, 1139 (2010).
- [10] Y. J. He, D. Mihalache, B. B. Hu, J. Opt. Soc. Am. B **27**, 2174 (2010).
- [11] C. P. Yin, D. Mihalache, Y. J. He, J. Opt. Soc. Am. B **28**, 342 (2010).
- [12] J. Lega, J. V. Moloney, A. C. Newell, Phys. Rev. Lett. **73**, 2978 (1994).
- [13] J. M. Soto-Crespo, N. Akhmediev, Phys. Rev. E Stat. Nonlin. Soft Matter Phys. **66**, 066610 (2002).
- [14] N. Akhmediev, A. Ankiewicz, Lect. Notes Phys. **661**, 1 (2005).
- [15] J. Buceta, K. Lindenberg, J. M. R. Parrondo, Phys. Rev. Lett. **88**, 024103 (2002).
- [16] D. A. Zezulín, Y. V. Kartashov, V. V. Konotop, Opt. Lett. **36**, 1200 (2011).
- [17] D. Mihalache, Rom. J. Phys. **59**, 295 (2014).
- [18] Y. J. He, B. A. Malomed, D. Mihalache, Phil. Trans. R. Soc. A **372**, 20140017 (2014).
- [19] V. J. Sánchez-Morcillo, K. Staliunas, Phys. Rev. E Stat. Phys. Plasmas Fluids Relat. Interdiscip. Topics **60**, 6153 (1999).
- [20] R. Driben, B. A. Malomed, A. Gubeskys, J. Zyss, Phys. Rev. E. **76**, 066604 (2007).
- [21] J. Burke, E. Knobloch, Phys. Rev. E Stat, Nonlin. Soft Matter Phys. **73**, 056211 (2006).
- [22] V. Skarka, N. B. Aleksić, Phys Rev Lett. **96**, 013903 (2006).
- [24] V. Skarka, N. B. Aleksic, D. Gauthier, D. V. Timotijevic, Piers Online **3**, 83(2007).
- [25] G. P. Agrawal, Nonlinear Fiber Optics, 3rd ed., California: Academic Press, 2001.

*Corresponding author: jgy579@126.com